*Journal of Sound and Vibration* (1998) **215**(1), 167–181
*Article No*. sv981617

# COUPLED TORSIONAL AND BENDING VIBRATIONS OF DRILLSTRINGS SUBJECT TO IMPACT WITH FRICTION

A. S. YIGIT AND A. P. CHRISTOFOROU

*Department of Mechanical and Industrial Engineering*, *Kuwait University*, *P.O. Box* 5969, *Safat*, 13060 *Kuwait*

(*Received* 8 *January* 1998, *and in final form* 13 *March* 1998)

A dynamic model for coupled torsional and bending vibrations of drillstrings is presented. The bit/formation interactions are assumed to be related to the bit motion, leading to a set of highly non-linear equations with a potential for self-excited behaviour. Impacts with the borehole wall are accounted for by a consistent contact model which is capable of capturing rolling both with and without slip of the drill collars along the borehole wall. Simulation results show that the non-linear coupling significantly affects the response. Due to the combined parametric and forcing excitations and the effect of strong non-linearities, the response is not simple or easily predictable. At certain frequencies, there is significant energy transfer between the two modes of vibrations. The simulation results agree well with laboratory and field observations when the so called stick–slip vibrations occur. This study suggests a new mechanism for this behaviour which was shown to be due to static friction or speed dependent torque on bit.



## 1. INTRODUCTION

It is well known that drillstring vibrations may lead to fatigue failures and abrasive wear of tubulars, damage to the drill bit and the borehole wall. As a consequence, oilwell drilling becomes inefficient and costly. On the other hand, measurements of these vibrations may provide valuable information about the drilling assembly and formation characteristics. Therefore, vibrations must be fully understood and their effects should be minimized in any approach to drilling optimization.

Drillstring vibrations are generally quite complex. Axial, lateral and torsional vibrations are all present and coupled. Phenomena such as bit bounce, stick–slip, forward and backward whirl and parametric instabilities have all been shown to occur. Because of the complexity, a full simulation covering all relevant phenomena is not practical, and a common approach has been to study vibration mechanisms individually [1–5].

Some studies on drillstring dynamics were mostly concerned with axial and torsional vibrations. The coupling between these two motions was also noted [1]. Later, it was shown that the coupling mechanism between axial and torsional vibrations can lead to large torsional vibrations [6]. Kyllingstad and Halsey [7] studied the stick–slip vibrations due to static friction at the bit/formation interface. Brett [8] showed that the dependence of bit torque on the bit speed may also cause similar vibrations. Halsey *et al*. [9], have shown that torque feedback can help eliminate stick–slip vibrations. Another instability mechanism for coupled axial and torsional vibrations was proposed by Elsayed *et al*. [10] which is due to variation in the phase angle between surface undulations of subsequent cutters.

0022–460X/98/310167 + 15 $30.00/0 

Lateral vibrations which occur in the forms of whirling and parametric resonance have also been studied extensively [11–16]. In these studies, the torsional vibrations are not considered and the drillstring is assumed to rotate at a constant speed. Consequently, the excitation due to bit/formation interaction was assumed to be a prescribed function of time (i.e., a mono-frequency harmonic excitation). In the current work, however, the full coupling between torsional and lateral vibrations is considered and the excitation at the bit is assumed to be related to the rotation of the bit. This makes the coupling between the torsional and bending vibrations much stronger and non-linear. Furthermore, a consistent impact model is used to account for impacts of drill collars with the borehole wall which may involve rolling with and without slip. The results show that the torsional vibrations can significantly affect the dynamic behaviour. The findings are in qualitative agreement with laboratory and field observations.

## 2. EQUATIONS OF MOTION

The equations of motion for coupled torsional and bending vibrations are obtained through a simplified model with equivalent lumped parameters shown in Figure 1. The stabilized portion of the Bottom Hole Assembly (BHA) is modelled as a simply supported shaft for the transverse motion of the drill collars and the whole drillstring is assumed to be fixed at the top and free at the bit for torsional motion. The BHA is assumed to be rigid with respect to torsional vibrations since the drill collars are much stiffer than the drill pipe. By applying Newton's law in polar co-ordinates attached to the borehole centre, the following equations are obtained:

$$(m+m_f)(\ddot{r}-r\dot{\theta}^2)+k(\phi)r+c_h|\mathbf{v}|\dot{r}=(m+m_f)e_0[\dot{\phi}^2\cos(\phi-\theta)+\ddot{\phi}\sin(\phi-\theta)]-F_r, \tag{1}$$

$$(m+m_f)(r\ddot{\theta}+2\dot{r}\dot{\theta})+c_h|\mathbf{v}|r\dot{\theta}=(m+m_f)e_0[\dot{\phi}^2\sin(\phi-\theta)-\ddot{\phi}\cos(\phi-\theta)]+F_\theta, \tag{2}$$

$$J\ddot{\phi}+k_T(\phi-\phi_{rot})+c_v\dot{\phi}+c_h|\mathbf{v}|\dot{r}e_0\sin(\phi-\theta)-c_h|\mathbf{v}|r\dot{\theta}e_0\cos(\phi-\theta)$$
$$=-T(\phi)+F_\theta[R-e_0\cos(\phi-\theta)]-F_re_0\sin(\phi-\theta). \tag{3}$$

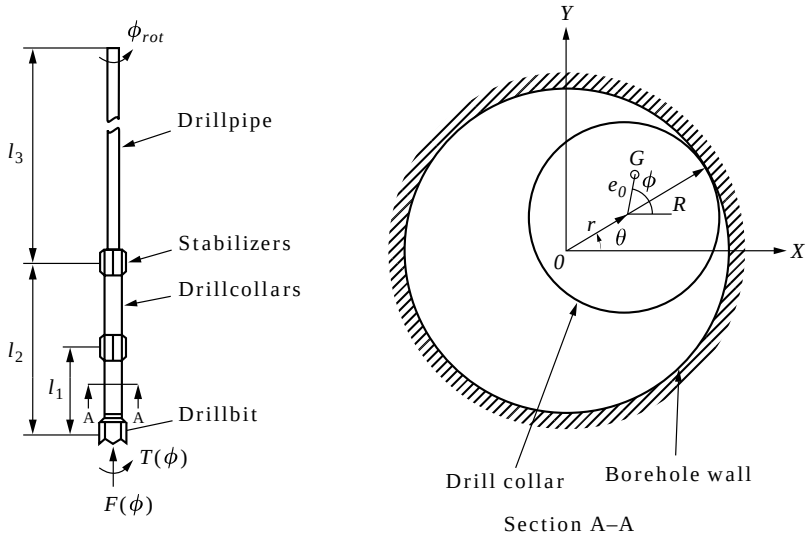


Figure 1. The sketch of the system.

TABLE 1

*Parameters used in the simulations*

| Drillstring | | Drilling mud | Borehole |
|---|---|---|---|
| $E = 210$ GPa | | $\rho_f = 1500$ kg/m$^3$ | $E = 210$ GPa |
| $\rho = 7850$ kg/m$^3$ | | $C_d = 1$ | $\rho = 7850$ kg/m$^3$ |
| $d_o = 0{\cdot}2286$ m | | $C_a = 1{\cdot}7$ | $d_h = 0{\cdot}4286$ m |
| $d_i = 0{\cdot}0762$ m | | $\mu_f = 0{\cdot}2$ Ns/m$^2$ | $\mu = 0{\cdot}3$ |
| $e_0 = 0{\cdot}0127$ m | | | $S_y = 600$ MPa |
| $l_1 = 19{\cdot}81$ m, | $l_2 = 200$ m | | |
| $l_3 = 1000$ m | | | |
| $\bar{d}_o = 0{\cdot}127$ m, | $\bar{d}_i = 0{\cdot}095$ m | | |
| Weight and torque on bit | | | |
| $P_0 = 100$ kN, | $P_f = 100$ kN; | $T_0 = 4$ kNm, | $T_f = 4$ kNm |

Here $\phi_{rot}$ is the angular displacement at the rotary table (top of the drillstring), $\phi$ is the angle of rotation of the drill collars, $\mathbf{v}$ is the velocity of the geometric centre of the drill collar section, $e_0$ is the eccentricity of the centre of mass with respect to the geometric centre of the collar section, $J$, $m$, $m_f$, $k(\phi)$, $k_T$, $c_h$ and $c_v$ are the equivalent mass moment of inertia, mass, added fluid mass, transverse stiffness, torsional stiffness, and hydrodynamic and viscous damping coefficients which are derived from the associated continuous model of the drill string by using a Lagrangian approach (see Appendix A), and $R$ is the radius of

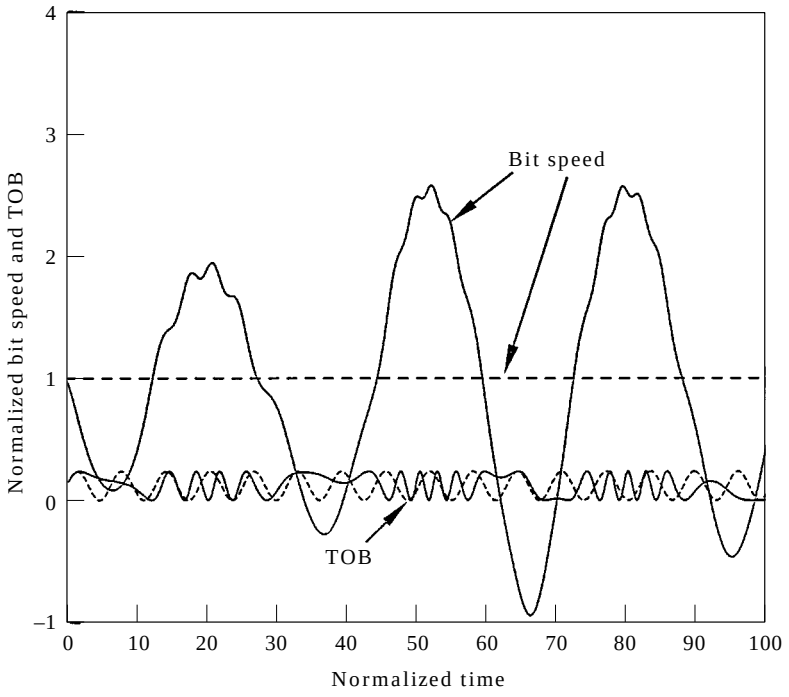


Figure 2. Effect of torsional vibrations on the bit speed and the TOB; ——, with torsion; – – –, without torsion.

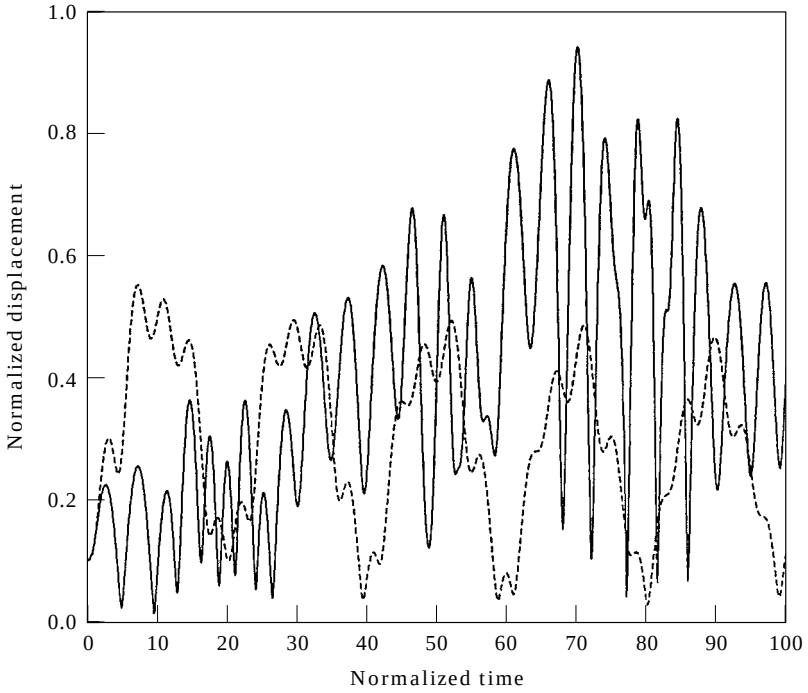


Figure 3. Effect of torsional vibrations on the lateral vibration; key as Figure 2.

the drill collars. In the present study, the angular velocity of the rotary table is assumed to be given as

$$\omega(t) = \omega_0 + \omega_a \sin \omega_r t, \tag{4}$$

where $\omega_0$ is the prescribed angular velocity of the rotary table, and $\omega_a$ and $\omega_r$ are the amplitude and the frequency of angular velocity fluctuations which depend on the control characteristics of the rotary table drive system. By integrating equation (4) with respect to time, the angular displacement of the rotary table can be obtained as

$$\phi_{rot} = \omega_0 t + (\omega_a/\omega_r)(1 - \cos \omega_r t). \tag{5}$$

It should be noted that with the model described above, the rotary speed at the bit will not be the same as the rotary table speed since it is one of the degrees of freedom of the system. Consequently, the excitation forces due to the bit/formation interactions are no longer prescribed functions of time as commonly assumed [1–5, 11–16]. Therefore, the torque on bit (TOB), $T(\phi)$, and the weight on bit (WOB), $F(\phi)$ are assumed to be

$$T(\phi) = T_0 + T_f \sin n\phi, \qquad F(\phi) = F_0 + F_f \sin n\phi, \tag{6, 7}$$

where $n$ is the bit factor which depends on the type of the bit used, and, the subscripts 0 and $f$ denote the mean and the amplitude values, respectively. The only continuous external dynamic excitation comes from the prescribed motion of the rotary table. As a consequence, linear phenomena such as simple and parametric resonance [14, 15], and whirling [11–13], which are based on the assumption of harmonic excitations, are not straightforward. Other intermittent external excitations are $F_r$ and $F_\theta$ which are the radial and transverse contact forces, respectively, resulting from impacts of the drill collars with the borehole wall. When there is no contact between the collars and the borehole wall, these forces are zero.

## 3. ANALYSIS OF CONTACT WITH THE BOREHOLE WALL

Previously, the impact between the drill collars and the borehole wall was modelled through a linear or Hertzian contact stiffness [13, 16]. In these studies the effect of friction was accounted for with the assumption of continuous sliding between the two surfaces. Clearly, there might be situations where the collars roll along the borehole wall without slip. In this study, to account for this type of contact situations, a different impact model is used. This impact model is based on the impulse–momentum principle and it is assumed that the impact is instantaneous [17, 18].

The impulse–momentum equations are obtained by integrating equations (1)–(3) with respect to time during the contact duration $\Delta t = t_2 - t_1$:

$$\int_{t_1}^{t_2} \{(m + m_f)(\ddot{r} - r\dot{\theta}^2) + k(\phi)r + c_h|\mathbf{v}|\dot{r}\}\, \mathrm{d}t$$

$$= \int_{t_1}^{t_2} \{(m + m_f)e_0[\dot{\phi}^2 \cos(\phi - \theta) + \ddot{\phi} \sin(\phi - \theta)] - F_r\}\, \mathrm{d}t, \tag{8}$$

$$\int_{t_1}^{t_2} \{(m + m_f)(r\ddot{\theta} + 2\dot{r}\dot{\theta}) + c_h|\mathbf{v}|r\dot{\theta}\}\mathrm{d}t$$

$$= \int_{t_1}^{t_2} \{(m + m_f)e_0[\dot{\phi}^2 \sin(\phi - \theta) - \ddot{\phi} \cos(\phi - \theta)] + F_\theta\}\, \mathrm{d}t, \tag{9}$$

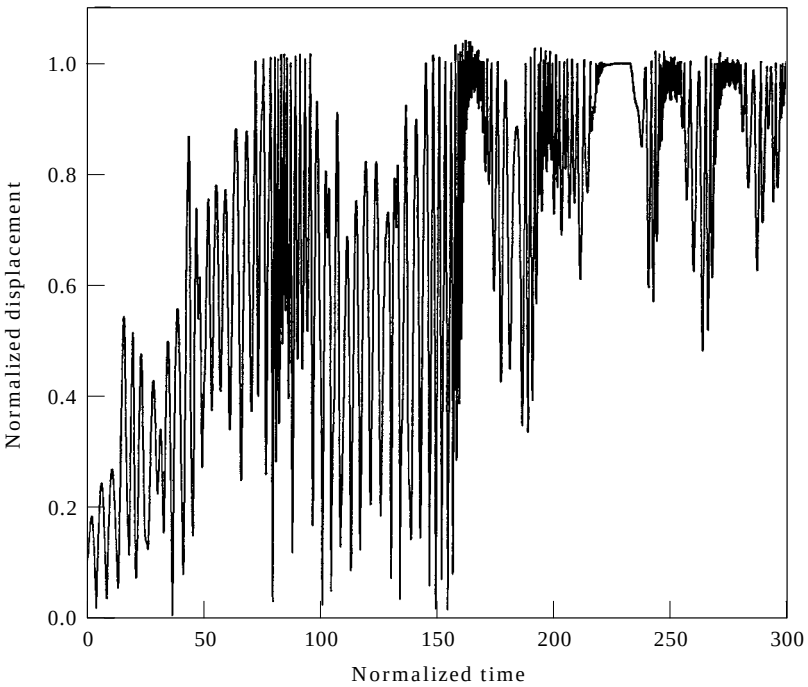


Figure 4. Lateral vibrations with impacts with the borehole wall.

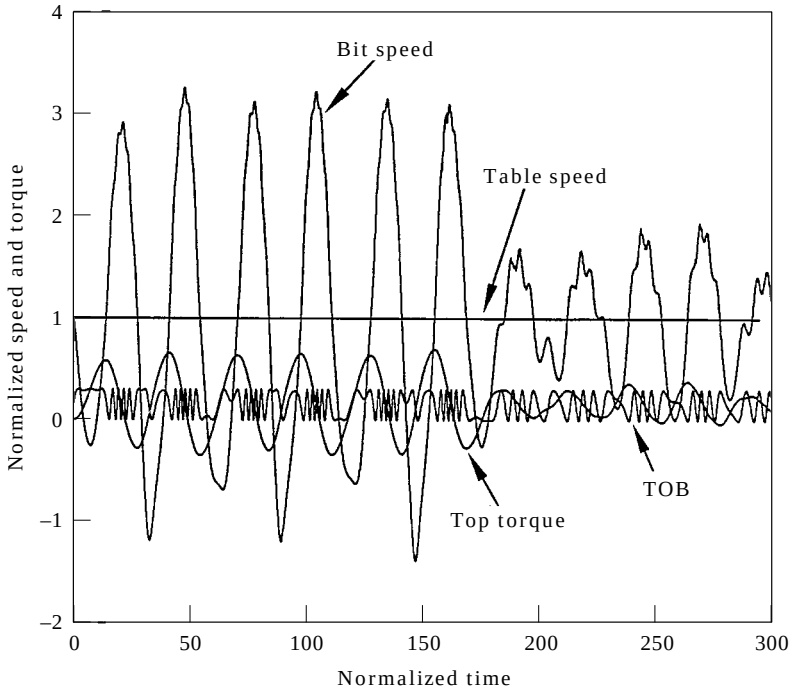


Figure 5. Torsional vibrations with impacts with the borehole wall.

$$\int_{t_1}^{t_2} \{J\ddot{\phi} + k_T(\phi - \phi_{rot}) + c_v\dot{\phi} + c_h|\mathbf{v}|\dot{r}e_0 \sin(\phi - \theta) - c_h|\mathbf{v}|r\dot{\theta}e_0 \cos(\phi - \theta)\}\, \mathrm{d}t$$

$$= \int_{t_1}^{t_2} \{-T(\phi) + F_\theta[R - e_0 \cos(\phi - \theta)] - F_r e_0 \sin(\phi - \theta)\}\, \mathrm{d}t. \tag{10}$$

As the contact duration approaches zero, which is the main assumption here, and upon noting that the system configuration is continuous, equations (8)–(10) can be shown to yield the momentum balance equations [17]

$$(m + m_f)\Delta\dot{r} = -P_r + (m + m_f)e_0\Delta\dot{\phi} \sin(\phi - \theta), \tag{11}$$

$$(m + m_f)r\Delta\dot{\theta} = P_\theta - (m + m_f)e_0\Delta\dot{\phi} \cos(\phi - \theta), \tag{12}$$

$$J\Delta\dot{\phi} = [R - e_0 \cos(\phi - \theta)]P_\theta - e_0 \sin(\phi - \theta)P_r, \tag{13}$$

where $\Delta\dot{r}$ and $\Delta\dot{\theta}$ are the jump discontinuities in the velocities, and $P_r$ and $P_\theta$ are the impulses in radial and transverse directions, respectively, defined as

$$P = \lim_{\Delta t \to 0} \int_{t_1}^{t_2} F(t)\, \mathrm{d}t. \tag{14}$$

The radial and transverse impulse values for a particular impact are calculated by using the two-dimensional rigid-body impact-friction model proposed by Wang and Mason [19]. For completeness, the details of this model as applied to the system studied here are given in Appendix B.

The response of the system before an impact is obtained by numerical integration of the equations of motion (equations (1)–(3)). At each integration time step, the contact conditions are checked by using a contact algorithm. If an impact is detected to occur, the integration is stopped and the momentum balance equatons (equations (11)–(13)) are formed and solved for the jump discontinuities in velocities. Then, the integration is restarted again with the new initial conditions.

## 4. DIMENSIONLESS FORMULATION

For convenience, the governing equations are expressed in dimensionless form by defining the variables

$$\tau = \omega_0 t, \qquad \bar{r} = r/b_c, \tag{15}$$

where $b_c$ is the clearance between the borehole wall and drill collar. Substitution of equations (15) into equations (1)–(3) lead to the dimensionless equations

$$\ddot{\bar{r}} + \bar{\omega}_b^2(1 - \varepsilon \sin n\phi)\bar{r} + \bar{c}_h|\mathbf{v}|\dot{\bar{r}} - \bar{r}\dot{\theta}^2 = \bar{e}_0\dot{\phi}^2 \cos(\phi - \theta) + \bar{e}_0\ddot{\phi} \sin(\phi - \theta) - \bar{F}_r, \tag{16}$$

$$\bar{r}\ddot{\theta} + 2\dot{\bar{r}}\dot{\theta} + \bar{c}_h|\bar{\mathbf{v}}|\bar{r}\dot{\theta} = \bar{e}_0\dot{\phi}^2 \sin(\phi - \theta) - \bar{e}_0\ddot{\phi} \cos(\phi - \theta) + \bar{F}_\theta, \tag{17}$$

$$\ddot{\phi} + \bar{\omega}_s^2(\phi + \phi_f \sin n\phi) + 2\zeta\bar{\omega}_s\dot{\phi} + \bar{c}_h^*|\bar{\mathbf{v}}|[\dot{\bar{r}} \sin(\phi - \theta) - \bar{r}\dot{\theta} \cos(\phi - \theta)]$$
$$= \bar{\omega}_s^2(\phi_{rot} - \phi_0) + \bar{T}_\theta[R - \bar{e}_0 \cos(\phi - \theta)] + \bar{T}_r\bar{e}_0 \sin(\phi - \theta), \tag{18}$$

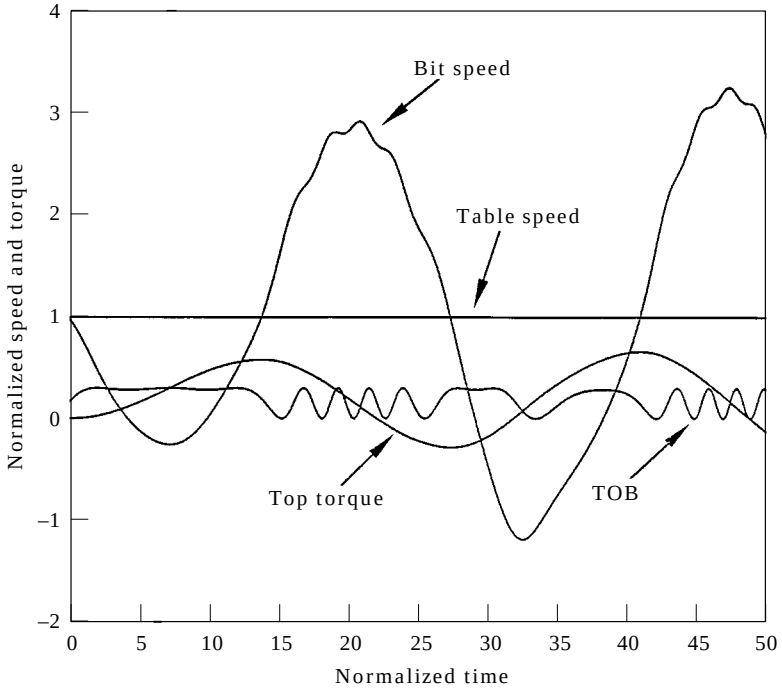


Figure 6. Torsional vibrations with impacts with the borehole wall (close-up view).

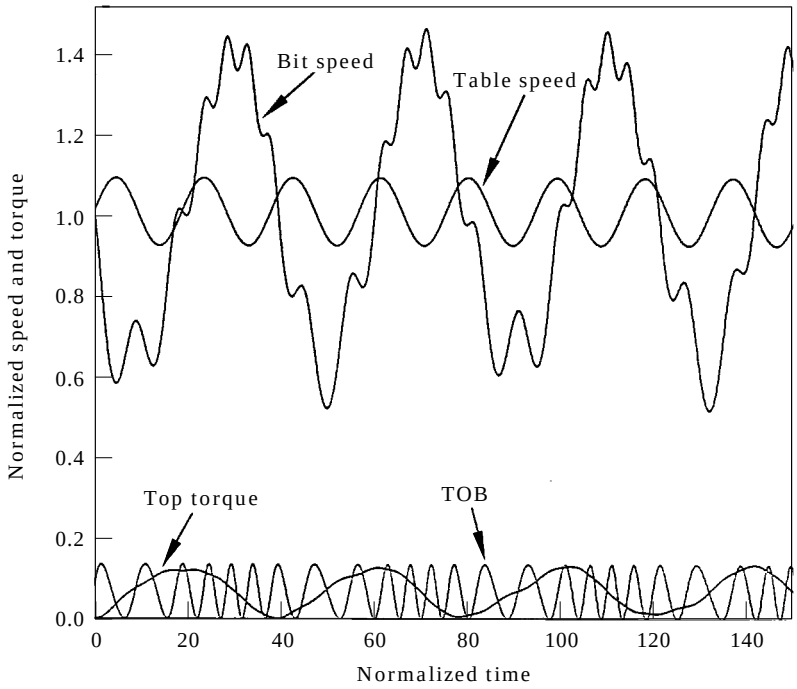


Figure 7. Torsional vibrations with a fluctuating table speed.

with the following dimensionless parameters:

$$\bar{\omega}_b^2 = \frac{\omega_b^2}{\omega_0^2}\left(1 - \frac{\pi T_0}{l_1 F_{cr}} - \frac{F_0}{F_{cr}}\right), \qquad \varepsilon = \frac{\pi T_f + l_1 F_f}{l_1 F_{cr} - \pi T_0 - l_1 F_0}, \tag{19}$$

$$\bar{F}_r = \frac{F_r}{(m + m_f) b_c \omega_0^2}, \qquad \bar{F}_\theta = \frac{F_\theta}{(m + m_f) b_c \omega_0^2}, \tag{20}$$

$$\bar{T}_\theta = F_\theta b_c / J\omega_0^2, \qquad \bar{T}_r = F_r b_c / J\omega_0^2, \tag{21}$$

$$\bar{e}_0 = e_0 / b_c, \qquad \bar{R} = R / b_c, \tag{22}$$

$$\bar{c}_h = c_h b_c / (m + m_f), \qquad \bar{c}_h^* = c_h b_c^2 e_0 / J, \tag{23}$$

$$\bar{\omega}_s = \omega_s / \omega_0, \tag{24}$$

$$\zeta = c_v / 2J\omega_s, \qquad \phi_0 = T_0 / k_T, \qquad \phi_f = T_f / k_T. \tag{25}$$

Here $\omega_b$ and $\omega_s$ are the natural frequencies for bending and torsion of the unloaded drillcollar for the associated linear uncoupled problem, respectively, and $F_{cr}$ is the Euler buckling load given as

$$\omega_b^2 = EI\pi^4 / 2(m + m_f) l_1^3, \qquad \omega_s^2 = k_\tau / J, \qquad F_{cr} = \pi^2 EI / l_1^2, \tag{26}$$

It is clear that equations (16)–(18) constitute a highly non-linear coupled set of ordinary differential equations as opposed to differential equations with time varying coefficients used in previous studies. Since the excitation due to the bit/formation interaction is assumed to be related to the rotation of the bit the coupling between the torsional and bending vibrations is much stronger. Therefore, it is expected that when the torsional

vibrations are excited, they will play a dominant role in the dynamic behaviour of drillstrings. In the following section a number of simulations are presented to demonstrate the use of the proposed model in predicting the dynamic behaviour.

## 5. SIMULATION RESULTS AND DISCUSSION

The dynamic response of a drillstring is obtained by a numerical solution of equations (16)–(18) with appropriate initial conditions until an impact occurs with the borehole wall. The effect of impact on the response is accounted for by using the momentum balance method described in section 3. Because of impacts and other non-linearities, a numerical solution procedure based on a variable-step variable-order predictor–corrector differential equation solver, which is suitable for stiff problems, is used to integrate the equations of motion [20]. As is well known, the accuracy of the numerical solution depends on the choice of the time step. As a rule of thumb, the time step used was 1/10 of the smallest natural period of the associated linear problem. In addition, the time step is reduced internally in the integrator to avoid discontinuities in the response. The time step is reduced by ten times if the relative error bound specified ($10^{-8}$) is exceeded. This is especially important in order to handle chatter-like behaviour.

The parameters used in the following simulations are shown in Table 1, and represent a typical case in oil well drilling operations. The rotary table speed is varied between 6 and 15 rad/s which is a common operating range. From a simple linear and uncoupled analysis for this set-up, the critical frequency for torsional resonance is found to be 1·85 rad/s, while the critical frequency for whirling resonance (due to bending) is found to be 6·14 rad/s. Since whirling has been investigated earlier [11–13, 16], only the simulations showing the effects of torsional vibrations are presented in this paper.

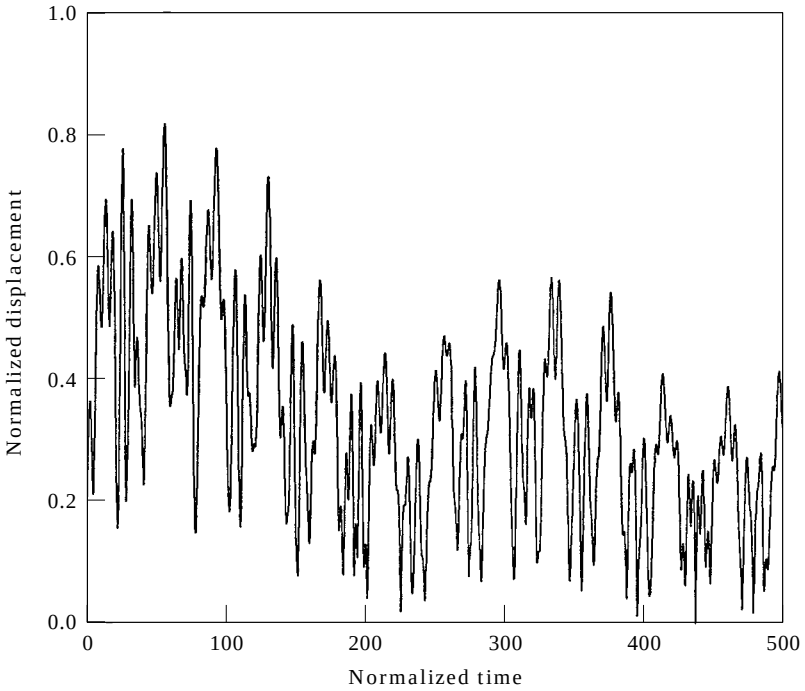


Figure 8. Lateral vibrations with a fluctuating table speed.

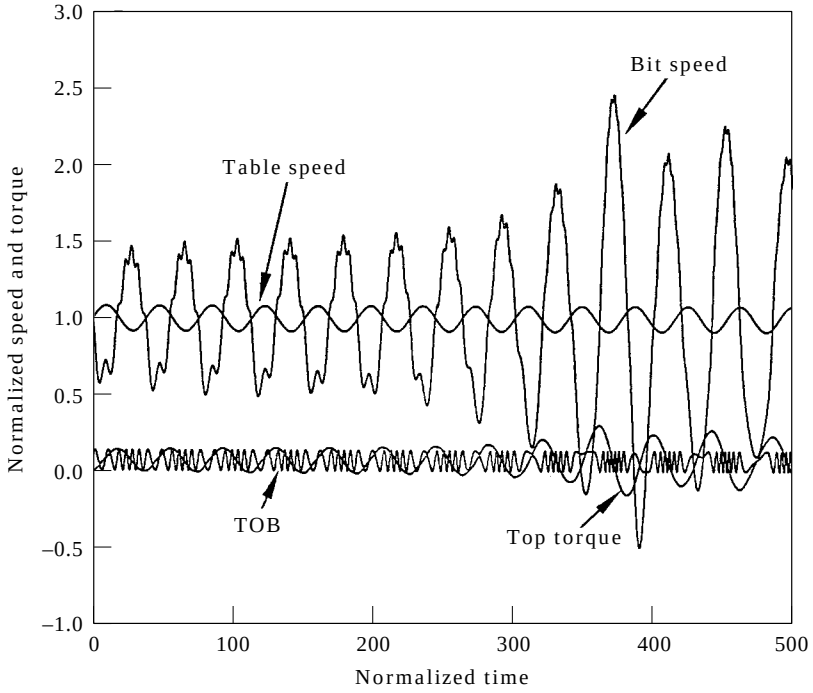


Figure 9. Torsional resonance due to fluctuating table speed.

In the first set of simulations, which are shown in Figures 2–5, the rotary table speed is assumed to be constant. This assumption has been commonly used in most drilling dynamics studies [1–5, 11–16]. Figures 2 and 3 show the effect of torsional vibrations on the bit speed, Torque On Bit (TOB), and lateral vibrations when the rotary table speed is equal to 9 rad/s. As clearly seen in Figure 2, when torsional vibrations are not considered, the bit speed is the same as the rotary table speed, and the TOB is a pure sinusoid. In other words, the bit speed and the TOB are completely prescribed, which is generally the approach taken in most earlier studies dealing with lateral vibrations of drillstrings [15, 16]. When there are considerable torsional vibrations, however, the bit speed is significantly different from the rotary table speed. In fact, field measurements have shown that, when there are significant torsional vibrations, the bit speed differs from the rotary table speed by as much as three times [8, 9], which is also in agreement with the present results. As a consequence, the TOB time history contains finite time intervals during which the bit is non-rotating (constant $\phi$) followed by high frequency oscillations. This type of behaviour is an indication of stick-slip motion which will be examined later with further simulations. As expected, the torsional vibrations also affect the lateral vibrations, as is clearly seen in Figure 3. With the bit speed reaching almost three times the rotary table speed, because of the rotating unbalance, the amplitudes of transverse vibrations are much higher. Note that the rotary table speed of 9 rad/s is away from any linear critical speed for either torsional or lateral vibrations. Apparently, the non-linear coupling between torsional and lateral vibrations complicates the dynamics, and requires further investigation.

Figures 4 and 5 show the dynamic response when the rotary table speed is equal to 8 rad/s. The lateral vibrations shown in Figure 4 indicate an unstable response and consequently, impacts with the borehole wall occur. As can be seen, in addition to impacts

there may be periods of continuous rubbing and rolling along the borehole wall. It should be noted that the impact model used is instrumental in capturing this type motion accurately. The instability of the response can also be seen in the torsional vibrations shown in Figure 5. Since the growth of amplitudes are far from being linear it is probable that parametric resonance occurs due to the non-linear stiffness term in equation (18). It seems that the growth of torsional vibrations lead to large lateral vibrations and impacts. Impacts with friction, however, reduce the torsional vibrations, and the torsional instability manifests itself in the lateral vibrations, and energy is transferred from torsional to lateral motion.

The effect of large torsional vibrations on the TOB is also evident in Figure 5. As mentioned earlier, when the torsional vibrations are significant, the stick–slip behaviour is observed in the TOB time history. When the torsional vibrations are reduced due to impacts, the TOB becomes a pure sinusoid. In order to investigate the motion of the bit further, a close-up view of Figure 5 is shown in Figure 6. It is seen that when the bit speed is approaching zero, the TOB trace is becoming flat, indicating a sticking behaviour. Each flat region is followed by a sinusoidal pattern whose frequency varies according to the bit speed. During this period, the drill pipe is twisted by the rotary table causing the surface torque to increase as shown in Figure 6. This is followed by a release of the torsional energy stored during the sticking period causing the bit to speed up to more than twice the rotary table speed before it slows down and again comes to a complete stop. The period of these alternating modes of relaxation and torsion is approximately equal to the period of torsional vibrations. The field data observed by Halsey *et al*. [9] closely resembles the results presented in Figure 5. This is interesting, because in this study there are no externally prescribed stick–slip conditions at the bit/formation interface. Instead, this behaviour is the result of the model used for TOB and is entirely due to the coupled

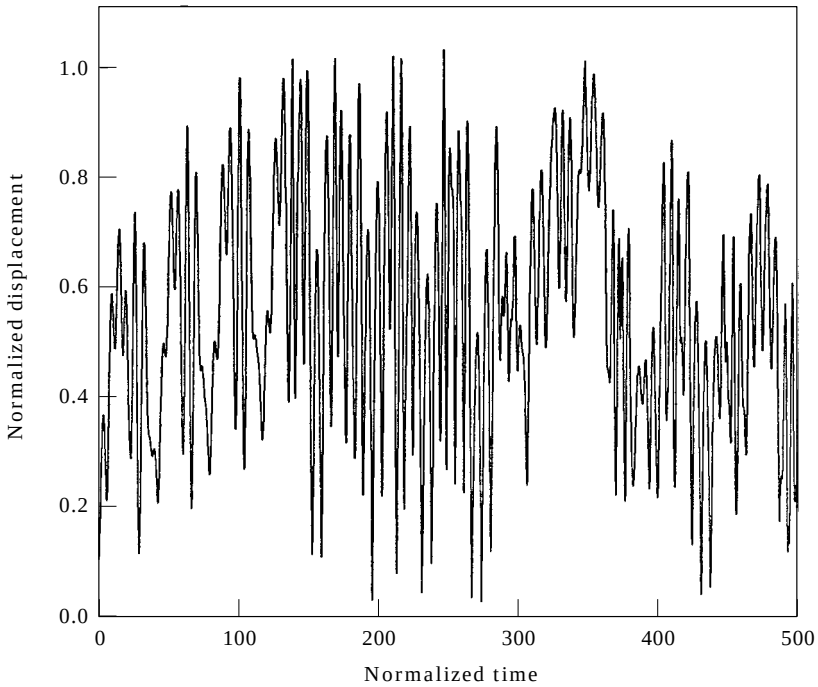


Figure 10. Unstable lateral vibrations with a fluctuating table speed.

dynamics rather than Coulomb friction alone. It is worth noting that the results presented here may explain some of the observed stick–slip vibrations with tricone bits.

Since no speed control system is perfect some fluctuation in the rotary table speed is inevitable. In fact, there are field observations showing a sinusoidally varying table speed [8]. It is therefore, important to investigate the effect of these speed fluctuations on the coupled dynamics. The results of this investigation are shown in Figures 7–10. Figures 7 and 8 show a typical response when the nominal table speed is 12 rad/s. The amplitude and the frequency of the speed fluctuation are 1 rad/s and 4 rad/s, respectively. In this case the table and the bit speeds are very similar to the ones observed by Brett [8] with some small harmonics present in the bit speed which is due to the coupling with the lateral vibrations. Figures 9 and 10 show the response when the frequency $\omega_r$ is decreased to 2 rad/s, which is close to the linear torsional natural frequency (1·846 rad/s). As can be seen in Figure 9, the growing torsional vibration amplitudes indicate a resonance behaviour. The instability in the torsional vibrations leads to growing lateral amplitudes and eventual impacts with the borehole wall, as seen in Figure 10. As in the case of parametric instability presented in Figures 4 and 5, the energy responsible for the large lateral motion is derived from the torsional vibrations which are reduced due to friction with the borehole wall.

As demonstrated, the model presented here can be used to predict the coupled response of drillstrings for a particular set of operating conditions. It has been found that torsional vibrations have a strong influence on the lateral instabilities. Since the torsional vibrations can be measured easily at the surface, the coupled model can be used to monitor and control the downhole vibrations. The results of the current study explain clearly why the stick–slip vibrations are eliminated with a torque feedback [8, 9]. Surface torque is a measure of torsional vibrations, and controlling this torque is equivalent to controlling the torsional vibrations. When the torsional vibrations are small, there are no stick–slip vibrations. Furthermore, reducing the torsional vibrations will eliminate a number of instabilities, thus leading to smoother drilling.

## 6. CONCLUSIONS

A dynamic model for studying coupled torsional and bending vibrations of drillstrings has been presented. In the proposed model the WOB and the TOB are assumed to be functions of the bit rotation. Consequently, the torsional vibrations affect these excitations leading to self-excited behaviour. The impacts with the borehole wall are accounted for by using the momentum balance method with appropriate coefficients of restitution and friction. The impact model is capable of capturing both rolling with and without slip of the drill collars along the borehole wall.

It has been shown that the non-linear coupling significantly affects the response. Instabilities may occur at rotary speeds which may not be considered critical from an uncoupled linear analysis. At certain frequencies, there is significant energy transfer between the two modes of vibrations. The simulation results are in qualitative agreement with laboratory and field observations when the so called stick–slip vibrations occur. This study suggests a new mechanism for this behaviour which has been shown to be due to static friction or speed dependent TOB. It also explains why controlling the surface torque instead of rotary table speed eliminates stick–slip vibrations. The model proposed can be used for predicting the non-linear dynamics as well as controlling the coupled bending and torsional vibrations in drillstrings.

## ACKNOWLEDGMENT

This work was supported by Kuwait University, Research Administration, Grant Number EM-122.

## REFERENCES

1. I. Finnie and J. J. Bailey 1960 *American Society of Mechanical Engineers Journal of Engineering for Industry*, **May**, 129–135. An experimental study of drillstring vibration.
2. P. R. Paslay and D. B. Bogy 1963 *American Society of Mechanical Engineers Journal of Engineering for Industry*, **May**, 187–194. Drill string vibrations due to intermittent contact of bit teeth.
3. D. W. Dareing and B. Livesay 1968 *American Society of Mechanical Engineers Journal of Engineering for Industry*, **October**, 1–9. Longitudinal and angular drillstring vibrations with damping.
4. R. F. Mitchell and M. B. Allen 1985 *World Oil*, **March**, 101–104. Lateral vibration: the key to BHA failure analysis.
5. J. Kaski 1993 *Proceedings of the* 14*th Biennial ASME Design Technical Conference on Vibration and Noise*, *Albuquerque*, *NM*, **DE-60**, 355–362. On the generation of bending vibration in a drill rod.
6. T. V. Aarrestad and A. Kyllingstad 1988 *Society of Petroleum Engineers Drilling Engineering* **3**, 12–18. An experimental and theoretical study of a coupling mechanism between longitudinal and torsional drillstring vibrations at the bit.
7. A. Kyllingstad and G. W. Halsey 1988 *Society of Petroleum Engineers Drilling Engineering* **3**, 369–373. A study of slip stick motion of the bit.
8. G. F. Brett 1992 *Society of Petroleum Engineers Drilling Engineering* **7**, 168–174. The genesis of torsional drillstring vibrations.
9. G. W. Halsey, A. Kyllingstad and A. Kylling 1988 *Proceedings of the* 63*rd Society of Petroleum Engineers Drilling Engineering Annual Technical Conference and Exhibition*, Houston *TX*, 277–282. Torque feedback used to cure slip–stick motion.
10. M. A. Elsayed, D. W. Dareing and M. A. Vonderheide 1997 *American Society of Mechanical Engineers Journal of Energy Resources Technology* **119**, 11–19. Effect of torsion on stability, dynamic forces, and vibration characteristics in drillstrings.
11. R. J. Shyu 1989 *Ph.D. Dissertation*, *Massachusetts Institute of Technology*, *Department of Ocean Engineering*, Bending vibrations of rotating drillstrings.
12. J. K. Vandiver, J. W. Nicholson and R. J. Shyu 1990 *Society of Petroleum Engineers Drilling Engineering* **5**, 282–190. Case studies of the bending vibration and whirling motion of drill collars.
13. J. D. Jansen 1991 *Journal of Sound and Vibration* **147**, 115–135. Non-linear rotor dynamics as applied to oilwell drillstring vibrations.
14. V. A. Dunayevsky, F. Abbassian and A. Judzis 1993 *Society of Petroleum Engineers Drilling and Completion* **8**, 84–92. Dynamic stability of drillstrings under fluctuating weight on bit.
15. A. Berlioz, J. Der Hogopian, R. Dufour and E. Draoui 1996 *American Society of Mechanical Engineers Journal of Vibration and Acoustics* **118**, 292–298. Dynamic behavior of a drill-string: experimental investigation of lateral instabilities.
16. A. P. Christoforou and A. S. Yigit 1997 *Journal of Sound and Vibration* **206**, 243–260. Dynamic modelling of rotating drillstrings with borehole interactions.
17. Y. A. Khulief and A. A. Shabana 1986 *Journal of Sound and Vibration* **104**, 187–207. Impact responses of multi-body systems with consistent and lumped masses.
18. A. S. Yigit and A. P. Christoforou 1998 *American Society of Mechanical Engineers Journal of Vibration and Acoustics* **120**, 47–53. The Efficacy of momentum balance method in transverse impact problems.
19. Y. Wang and M. T. Mason 1992 *American Society of Mechanical Engineers Journal of Applied Mechanics* **59**, 635–642. Two-dimensional rigid-body collisions with friction.
20. G. D. Byrne and A. C. Hindmarsh 1975 *AMC Transactions on Mathematical Software* **1**, 71–76. A polyalgorithm for the numerical solution of ordinary differential equations.
21. A. S. Yigit and A. P. Christoforou 1994 *Composite Engineering* **4**, 1143–1152. On the impact of a spherical indenter and an elastic-plastic transversely isotropic half-space.

## APPENDIX A: A LUMPED PARAMETER MODEL OF THE DRILLSTRING

The dynamics of a continuous structure can be described with a finite number of degrees of freedom if it is assumed that the displacements can be described as a superposition of finite number of modes. Equivalent system stiffness, damping and mass parameters for each mode of the simplified model can be obtained from the properties of the original structure by means of a virtual work approach. In this work, the stabilized section of the BHA is modelled as a simply supported beam for transverse motion of the collars, and the whole drillstring is assumed to be fixed at the top, and free at the bit for torsional motion. The BHA is assumed to be rigid for torsional vibrations. This assumption is justified since the drillcollars are much stiffer than the drill pipe in torsion. Assuming one mode approximation for both the transverse and torsional vibrations, the equivalent system parameters can be obtained as

$$J = 2\rho I l_2 + (1/3)\rho I_p l_3, \qquad m = \rho\pi(d_o^2 - d_i^2)l_1/8, \tag{A1, A2}$$

$$m_f = \pi\rho_f(d_i^2 + C_a d_o^2)l_1/8, \qquad k(\phi) = \frac{EI\pi^4}{2l_1^3} - \frac{T(\phi)\pi^3}{2l_1^2} - \frac{F(\phi)\pi^2}{2l_1}, \tag{A3, A4}$$

$$k_T = GI_p/l_3, \qquad c_h = (2/3\pi)\rho_f C_d d_o l_1, \qquad c_v = \pi\mu_f d_o^3 l_2/2(d_h - d_o), \tag{A5–A7}$$

where $\rho$, $E$ and $G$ are the density, Young's modulus, and shear modulus of the drillstring material, respectively, $I = \pi(d_o^4 - d_i^4)/64$ is the area moment of inertia for the cross-section, $d_o$ and $d_i$ are the outside and inside diameters of the drill collars, respectively, $\rho_f$ and $\mu_f$ are the density and the viscosity of the drilling mud, $C_a$ is the added mass coefficient due to the displaced mass of the mud inside the drillstring, $C_d$ is the drag coefficient for the hydrodynamic damping due to the mud, $d_h$ is the borehole diameter, $I_p = \pi(\overline{d}_o^4 - \overline{d}_i^4)/32$ is the polar area moment of inertia of the drill pipe section, and $\overline{d}_o$ and $\overline{d}_i$ are the outside and inside diameters of the drill pipe, respectively.

## APPENDIX B: IMPACT MODEL AND COEFFICIENT RESTITUTION

In impact of rigid bodies, the deformation history is assumed to consist of two phases: compression phase and restitution phase. The compression phase is the period from the instant of contact to the point of maximum compression when the relative approach velocity becomes zero. The restitution phase begins at the end of compression phase and ends at the instant of separation. In general, for an oblique impact, Mason and Wang [19] have identified five contact modes: (1) sliding, (2) sticking in compression phase (C-sticking), (3) sticking in restitution phase (R-sticking), (4) reversed sliding in compression phase (C-reversed sliding), and (5) reversed sliding in restitution phase (R-reversed sliding). By adopting the Poisson method for the coefficient of restitution, these contact modes and the associated radial and transverse impulses can be calculated. The necessary equations to calculate the impulses are as follows:

1. Sliding: if $P_d > (1 + e)P_q$,

$$P_r = -(1 + e)\frac{C_0}{B_2 + s\mu B_3}, \qquad P_\theta = -s\mu P_r; \tag{B1, B2}$$

2. C-sticking: if $P_d < P_q$ and $\mu > |\mu_s|$,

$$P_r = -(1 + e)\frac{B_1 C_0 + B_3 S_0}{B_1 B_2 - B_3^2}, \qquad P_\theta = \frac{B_3 P_r - S_0}{B_1}; \tag{B3, B4}$$

3. R-sticking: if $P_d < P_q < (1+e)P_q$ and $\mu > |\mu_s|$,

$$P_r = -(1+e)\frac{C_0}{B_2 + s\mu B_3}, \qquad P_\theta = \frac{B_3 P_r - S_0}{B_1}; \tag{B5, B6}$$

4. C-reversed sliding: if $P_d < P_q$ and $\mu < |\mu_s|$,

$$P_r = -\frac{1+e}{B_2 - s\mu B_3}\left[C_0 + \frac{2s\mu B_3 S_0}{B_3 + s\mu B_1}\right], \qquad P_\theta = s\mu\left[P_r - \frac{2S_0}{B_3 + s\mu B_1}\right]; \tag{B7, B8}$$

5. R-reversed sliding: if $P_d < P_q < (1+e)P_q$ and $\mu < |\mu_s|$,

$$P_r = -(1+e)\frac{C_0}{B_2 + s\mu B_3}, \qquad P_\theta = s\mu\left[P_r - \frac{2S_0}{B_3 + s\mu B_1}\right], \tag{B9, B10}$$

where

$$s = \begin{Bmatrix} S_0/|S_0| & \text{if } S_0 \neq 0 \\ 1 & \text{if } S_0 = 0 \end{Bmatrix}. \tag{B11}$$

Here $S_0$ and $C_0$ are the initial values of sliding and compression velocities calculated as

$$S_0 = r\dot{\theta} + R\dot{\phi}, \qquad C_0 = -\dot{r}, \tag{B12, B13}$$

$B_1$, $B_2$ and $B_3$ are constants which depend on the geometry and mass properties as

$$B_1 = 1/(m + m_f) + [R - e_0 \cos(\phi - \theta)]^2/J, \tag{B14}$$

$$B_2 = 1/(m + m_f) + [e_0 \sin(\phi - \theta)]^2/J, \tag{B15}$$

$$B_3 = e_0 \sin(\phi - \theta)[R - e_0 \cos(\phi - \theta)]/J. \tag{B16}$$

$P_d$, $P_q$ and $\mu_s$ are given as

$$P_d = (B_2 + s\mu B_3)sS_0, \qquad P_q = -(\mu B_1 + sB_3)C_0, \qquad \mu_s = -B_3/B_1. \tag{B17–B19}$$

Here $\mu$ and $e$ are the friction and restitution coefficients, respectively. The friction coefficient is assumed to be a constant which depends only on the properties of contacting materials, whereas the coefficient of restitution depends on the impact conditions as well as the material and geometric properties and is obtained from the contact law given in reference [21].

It was shown that the coefficient of restitution varies as

$$e = \begin{Bmatrix} 1 & \beta \leqslant 0{\cdot}893 \\ 0{\cdot}972\beta^{-1/4} & \beta > 0{\cdot}893 \end{Bmatrix}, \tag{B20}$$

where $\beta$ is the normalized impact velocity given as

$$\beta = \left(\frac{15{\cdot}735(m + m_f)(E^*)^4}{\pi^5 d_h^3 S_y^5}\right)^{1/2} \dot{r}, \tag{B21}$$

where $E^*$ is the effective Young's modulus for the contacting bodies given by

$$\frac{1}{E^*} = \frac{1 - \nu_1^2}{E_1} + \frac{1 - \nu_2^2}{E_2}, \tag{B22}$$

where $\nu_i$ and $E_i$ are the Poisson's ratio and Young's modulus for the drill collars and the casing/formation, respectively, and $S_y$ is the yield strength of the softer material.